**Tree Physiology** 30, 361–375
*doi:10.1093/treephys/tpp129*

# Hydraulic architecture and tracheid allometry in mature *Pinus palustris* and *Pinus elliottii* trees

C. A. GONZALEZ-BENECKE,[1,2] T. A. MARTIN[1] and G. F. PETER[1]

[1] *School of Forest Resources and Conservation, University of Florida, PO Box 110410, Gainesville, FL 32611-0410, USA*

[2] *Corresponding author (cgonzabe@ufl.edu)*

Received November 3, 2009; accepted December 21, 2009; published online January 26, 2010

**Summary** *Pinus palustris* Mill. (longleaf pine, LL) and *Pinus elliottii* Engelm. var. *elliottii* (slash pine, SL) frequently co-occur in lower coastal plain flatwoods of the USA, with LL typically inhabiting slightly higher and better-drained microsites than SL. The hydraulic architecture and tracheid dimensions of roots, trunk and branches of mature LL and SL trees were compared to understand their role in species microsite occupation. Root xylem had higher sapwood-specific hydraulic conductivity ($k_s$) and was less resistant to cavitation compared with branches and trunk sapwood. Root $k_s$ of LL was significantly higher than SL, whereas branch and trunk $k_s$ did not differ between species. No differences in vulnerability to cavitation were observed in any of the organs between species. Across all organs, there was a significant but weak trade-off between water conduction efficiency and safety. Tracheid hydraulic diameter ($D_h$) was strongly correlated with $k_s$ across all organs, explaining >73% of the variation in $k_s$. In contrast, tracheid length ($L_t$) explained only 2.4% of the variability. Nevertheless, for trunk xylem, $k_s$ was 39.5% higher at 20 m compared with 1.8 m; this increase in $k_s$ was uncorrelated with $D_h$ and cell-wall thickness but was strongly correlated with the difference in $L_t$. Tracheid allometry markedly changed between sapwood of roots, trunks and branches, possibly reflecting different mechanical constraints. Even though vulnerability to cavitation was not different for sapwood of roots, branches or the trunks of LL and SL, higher sapwood to leaf area ratio and higher maximum sapwood-specific hydraulic conductivity in roots of LL are functional traits that may provide LL with a competitive advantage on drier soil microsites.

*Keywords: hydraulic conductivity, vulnerability to cavitation, wood anatomy.*

## Introduction

One of the most extensive terrestrial ecosystem types in the southeastern US coastal plain is pine flatwoods, low-lying forests established on Pleistocene sand deposits (Ewel 1990). In pine flatwoods, the two dominant tree species are longleaf pine (*Pinus palustris* Mill.) and slash pine (*Pinus elliottii* Engelm. var. *elliottii*). Longleaf pine (LL) and slash pine (SL) overlap on mesic sites that occupy sandy, seldom inundated flatlands. However, LL typically dominates on drier better-drained sites that are slightly elevated and SL dominates on lower wetter sites (Ewel 1990). For example, on flatwood sites with seasonal ponding and a sawgrass fringe, SL are primarily located surrounding or even inside the seasonal ponds, and LL dominates the higher areas between ponds (Peet 2006). Barnett and Sheffield (2005) report that characteristics of native SL habitats are poorly drained flatwoods and stream edges as well as seasonally flooded areas such as bays and swamps.

Trees have evolved as large and hydraulically complex organisms and, according to Tyree and Ewers (1991), in order to effectively look at trees as a whole functional organism, it is necessary to study their hydraulic architecture. Tyree and Zimmermann (2002) indicate that within-tree variation in hydraulic architecture ultimately controls whole-tree water relations. During severe drought, stomatal conductance declines and the water potential of the tree tends to follow that of soil. Under water stress, plants also reduce their water supply to the leaves when their xylem conduits are cavitated, eventually reducing plant gas exchange (Hacke et al. 2000*b*), so vulnerability to cavitation may be coupled to stomatal closure (Tyree and Ewers 1991). Thus, xylem hydraulics and resistance to cavitation are important traits influencing drought resistance (Maherali et al. 2006). However, the mechanism(s) controlling within-tree variation in hydraulics are not well understood. For example, within tree organs, the variation in hydraulic architecture traits such as vulnerability to cavitation and sapwood-specific hydraulic conductivity and their linkage with xylem tracheid anatomy are important questions that remain unsolved.

To better understand these relationships, we compared whole-tree and organ sapwood-specific hydraulic conductivity, tracheid anatomy and vulnerability between SL that typically inhabit wetter zones and LL that dominates in higher and well-drained soils. We hypothesized that inter-specific differences in vulnerability to cavitation are associated with

this land distribution pattern, with SL being more vulnerable to cavitation than LL. We also hypothesize that within-tree variation in sapwood-specific hydraulic conductivity and vulnerability to cavitation are associated with changes in tracheid anatomy. To test these hypotheses, we measured plant hydraulic and xylem anatomical traits in co-occurring LL and SL in a mature flatwoods forest in north-central Florida, USA.

## Materials and methods

### *Site and stand description*

The study was carried out at the University of Florida's Austin Cary Memorial Forest, located 15 km northeast of Gainesville, FL, USA (29°44′ N latitude and 82°09′ W longitude). Soils are classified as poorly drained Pomona sands (sandy, siliceous, hyperthermic Ultic Aplaquods), with a discontinuous spodic horizon at 0.3–0.6 m depth and deeper argillic horizon at 1.0–1.4 m depth (Gaston et al. 1990). The 41-ha study stand consists of a naturally regenerated mixed LL and SL forest with trees from 25 to 85 years old, with a mean age of 65 years. Within the stand, SL tended to be clumped in the lower lying areas and along pond margins, all within a matrix of LL. At the time of measurement, stand basal area was 16.9 $m^2$ $ha^{-1}$, distributed as 73 and 17% LL and SL, respectively. The understory consisted of native species, dominated by gallberry (*Ilex glabra* (L.) Gray), saw palmetto (*Serenoa repens* (Bartr.) Small), wax myrtle (*Myrica cerifera* L.) and wiregrass (*Aristida stricta* Michx) (Powell et al. 2005).

### *Meteorological and soil moisture measurements*

Environmental information was recorded from April 2007 to August 2007 using an automatic weather station located on the top of a 30-m scaffolding tower, extended ~5 m above mean canopy height (Powell et al. 2005). All sensors were measured every 30 s with an automatic datalogger (CR10X, Campbell Scientific, Logan, UT, USA) and were stored as 30-min averages.

In April 2007, vertically oriented, 200-mm-long capacitive soil moisture probes (EC-20, Decagon Devices, Pullman, WA, USA) were installed at 50 and 150 cm depths to estimate volumetric soil water content ($\theta_v$) into two sectors representing the SL and LL pine microsites. The manufacturer's probe installation kit, consisting of a custom-shaped blade to make the insertion in the soil and a tool to place the probe into the insertion point, was used to install the probes. For deeper installations, an auger was used to reach the desired depth and then the installation kit with extension rods was used to install the probe. The soil volume measured by the probe was not disturbed. Estimations of water content for each probe were extrapolated to the mid-point distance between sensors. Soil-specific calibrations were developed from soil samples taken 50 cm away from each probe, but no difference with manufacturer's default calibration model was determined ($P = 0.65$ and 0.82 for intercept and slope, respectively). The model that transforms sensor outputs (mV) to volumetric water content used was: $\theta_v = -0.24508 + 0.0007958$ mV.

Soil matric potential ($\Psi_s$, MPa) was estimated for the 0.5-m-depth measurements using previous soil water retention curves generated for local Spodosols (H.L. Gholz, unpublished data) and for the 1.5-m-depth measurements using a computer program based on pedotransfer functions and parameterized with soil texture and bulk density data obtained at each location (Schaap et al. 2001; ROSETTA version 1.2, US Salinity Laboratory ARS–USDA, Riverside, CA, USA). Particle size distribution was determined using the hydrometer method (Gee and Bauder 1986). Soil bulk density (g $cm^{-3}$) was determined using a soil core sampler (0200, Soil Moisture Equipment Corp., Santa Barbara, CA, USA).

### *Tree selection*

Measurement trees were chosen from across the range of tree basal area using 'quantiles of total', a stratification scheme that weights the selection of large trees more heavily (Hatton et al. 1995, Martin et al. 1997, Čermák et al. 2004). Seven trees per species were selected for measurements of leaf water potential, sapflow, hydraulic conductivity, tracheid allometry, specific leaf area and leaf mass, but only four of those seven trees were felled for leaf area and trunk hydraulic properties measurements. Diameter at breast height (DBH) of selected trees averaged 326 and 348 mm, ranging between 198 and 418 mm and from 204 to 493 mm for LL and SL, respectively (Table 1). Average sapwood thickness was 52 and 69 mm, ranging between 39 and 66 mm and from 42 to 91 m for LL and SL, respectively.

### *Hydraulic conductivity and vulnerability to cavitation*

Between 18 April and 6 July 2007, a sample harvest was carried out on branches, roots and trunk in all selected trees. Hydraulic conductivity and air injection protocol to determine vulnerability curves on branches and roots segments has been described elsewhere (Sperry et al. 1988, Sperry and Saliendra 1994, Domec and Gartner 2001, Spicer and Gartner 2001). Hydraulic conductivity ($k$, $kg_{water}$ $s^{-1}$ $MPa^{-1}$ m) was calculated according to Darcy's law as the flow rate of water ($kg_{water}$ $s^{-1}$) for a given pressure gradient through a segment of known length (MPa $m^{-1}$) (Tyree and Zimmermann 2002). Sapwood-specific ($k_s$, $k$ $m^{-2}_{sapwood\ area}$ = $kg_{water}$ $s^{-1}$ $MPa^{-1}$ $m^{-1}$) and leaf-specific ($k_l$, $k$ $m^{-2}_{leaf\ area}$ = $kg_{water}$ $s^{-1}$ $MPa^{-1}$ $m^{-1}$ × $10^{-4}$) hydraulic conductivity was determined as $k$ divided by corresponding sapwood or leaf area distal to the segment (these were not calculated for roots due to unavailable data of sapwood area of root system of each tree). Leaf area distal to the branch segment was determined using needle mass and all-sided specific leaf area (SLA, $cm^2$ $g^{-1}$) measured for each sample. Sapwood area of each segment was determined by directly measuring the area on scanned sections cut with a razor blade on both ends of the sample using image analysis software (Image-Pro, Media Cybernetics, Carlsbad, CA, USA). Branches and roots were sampled early in the morning and im-

mediately wrapped with wet towels in plastic bags to prevent desiccation and stored in a cooler until measured; both types of samples were at least 1 m long. Branches were collected from the mid-crown using a self-propelled boom lift and pole pruner the same day of leaf water potential measurements (18 April 2007); roots were extracted from the upper 0.2–0.4-m-depth layer immediately after all branch measurements were completed (starting on 14 May and ending on 6 June 2007). For each tree, one sample was collected for branches and three samples were collected for roots, because of high variability in $k$ and vulnerability to cavitation in roots reported by Hacke et al. (2000*a*), and associated with differences in root diameter.

In the laboratory, organ segments (0.15–0.20 m in length and with xylem diameters of 2–12 mm) were cut underwater and fitted with both ends protruding into a 'Sperry tubing apparatus'. One end of the segment was attached to tubing filled with degassed and filtered (0.2 μm) water containing 20 mM KCl; no pH adjustments were performed (Pockman and Sperry 2000). The other end of the segment was attached to a tube filled with the same solution that had a 1-ml micropipette attached at the exit end, which conducted the efflux to a water reservoir on a balance (XA-100, Denver Instruments, Denver, CO, USA) connected to a computer. Water volume changes in the reservoir were determined using changes in weight measured to the nearest 0.0001 g every 10 s over a 5- to 10-min interval. As a solution reservoir and to control the hydrostatic pressure difference across the segment, a Mariotte tube was used (SMS, Tucson, AZ, USA), maintaining a hydraulic pressure head of 0.0075 MPa for all measurements. After the sample connection was made to the apparatus, flow into the segments without a pressure head ('background' flow) was measured before and after each gravimetric measurement (Davis et al. 1999, Pittermann and Sperry 2003). Background measurements were averaged and subtracted from regular gravimetric measurements to obtain a final $k$ value. Initial 'native' conductivity ($k_{nat}$) was determined as the first measurement immediately after sample collection (no more than 4 h after excision). After $k_{nat}$ determination, segments were soaked under vacuum for 48 h to refill embolized tracheids (Domec and Gartner 2001, Domec et al. 2005) with the same degassed and sterile filtered 20 mM KCl solution in order to estimate maximum conductivity ($k_{max}$).

At the time of leaf area harvesting (between 21 June and 9 July 2007), bole xylem segments were also collected. Hydraulic conductivity was measured using the 'pressure sleeve' apparatus as described by Spicer and Gartner (1998*a*, 1998*b*, 2001). From four trees selected for each species, harvest was conducted early in the morning to minimize tensions in the xylem. From each harvested tree, two 200–250-mm-tall cylinders were extracted using a chainsaw at the sapflow probe measurement height, one cylinder at ~1.8 m height ($S_{base}$) and the other cylinder at the crown base ($S_{crown}$). After the cylinder was cut, the sample was immediately wrapped with wet towels in plastic bags to prevent desiccation, stored in a cooler and transported to the laboratory for measurement. 'Native' conductivity measurements were conducted within 8 h of harvest. For each cylinder, at eight selected depths along the stem radius, wood xylem samples were extracted to determine the hydraulic conductivity radial profile (at 10, 20, 30, 40, 60, 80 and 100 mm depth, from outer to inner sapwood). In the case of the crown-base sample from small trees, only samples from 10 to 60 mm depth were extracted. Cylinders were first split with an axe, keeping the sample wet. Once the cylinder was split, the parts (with previously marked distal and proximal faces) were placed underwater and radial and tangential surfaces were obtained with 'corner chisels'. Samples of ~1 $cm^2$ size at the cross-sectional surface were extracted at the same depth as the sapflow measurements, more or less 50 mm circumferentially away from the adjacent sensor position. Still underwater, about 50–70 mm of each end of the sample was cut with chisel and razor blade, obtaining a final sample ~100 mm long.

A pressure sleeve apparatus was constructed following Spicer and Gartner (1998*a*) in order to seal the sides of the sample during hydraulic conductivity measurements. Samples were fitted inside the latex sleeve of the apparatus and air inside the chamber was pressurized to 0.1 MPa to hold the membrane against the sides to prevent leakage. Sealing was improved by adding silicon grease along radial walls of the sample before insertion into the latex sleeve. Water flows for native and maximum hydraulic conductivity were measured following the same procedure as was described for branches and roots. From each disk, $k_s$ weighted value was calculated using the formula:

$$k_s = \sum \frac{ks_i \cdot a_i}{a}$$

where $ks_i$ corresponds to the $k_s$ at depth $i$, $a_i$ is the area of the corresponding annulus at depth $i$ and $a$ is total sapwood area of the disk. In order to estimate $k_l$ at $S_{base}$ and $S_{crown}$, weighted $k_s$ was divided by total tree leaf area.

The vulnerability to cavitation curve (VC curve) was determined on all roots and branches; in the case of stem bole, VC curve was determined only on a sample extracted at a 20 mm depth, because most sapflow radial profiles measured in the same trees showed that midday sap flux density peaked close to that depth. The segments were placed, both ends protruding, in a double-ended pressure chamber, constructed with portable pressure chamber caps with compression gland cover (PMS Instrument Co., Corvallis, OR, USA) and a custom-designed aluminum body. In the case of branches, two shallow (0.5 mm deep) notches were cut into opposite sides of the xylem about 50 mm apart in the center of the segment in order to ensure entry of air into the xylem inside the pressure chamber; for root and trunk samples, notching was not necessary.

To obtain a VC curve, the chamber was first pressurized to 0.1 MPa for 10 min. Flow through the segment was stopped by closing the input valve. After pressurizing for 10 min, conductivity was measured until it stabilized (5–10 min). After this initial measurement, flow through the segment was reduced by closing the valve, and air pressure inside the chamber was increased to a prescribed value (0.5-MPa steps) and held for 10 min. Then air pressure was lowered back (depressurized) to 0.1 MPa for 3 min. Flow was re-introduced by opening

the valve and the hydraulic conductance re-measured. Exposure of the segment to progressively higher air pressures continued until hydraulic conductance measurements were at least 95% below the initial value. Before and after each $k$ measurement, 'background' flow rates were also determined.

For the trunk samples, segments were moved alternatively from the 'cavitation chamber' (where air injection was carried out) to the 'pressure sleeve' apparatus (where $k$ was measured); in the case of branches and roots, $k$ was measured inside the 'cavitation chamber'. A VC curve was later constructed for each segment showing the cumulative percentage decrease in hydraulic conductivity versus the negative of air-injection pressure applied. Percentage loss of conductivity (PLC) at a given pressure was calculated using the equation given by Sperry and Tyree (1988, 1990):

$$\mathrm{PLC}(\Psi) = \left(1 - \frac{k_{(\Psi)}}{k_{\max}}\right) \cdot 100$$

where PLC($\Psi$) is the percentage loss of conductivity at pressure $\Psi$, $k_{(\Psi)}$ is the hydraulic conductivity measured after applying pressure $\Psi$ and $k_{\max}$ is the maximum hydraulic conductivity previously measured after vacuum soaking. The plot of these data is the VC curve (Sperry and Tyree 1988). We used a sigmoidal equation (Pammenter and Vander Willinger 1998) to calculate biological parameters from the VC curve:

$$\mathrm{PLC}(\Psi) = \frac{100}{1 + e^{a \cdot (\Psi - b)}}$$

where $a$ is an indicator of the slope and $b$ represents the pressure applied at which 50% loss of conductivity occurred. As described by Domec and Gartner (2001), several parameters can be calculated in order to compare different curves:

$$\Psi_{50} = b$$

where $\Psi_{50}$ is the xylem tension (MPa) at which 50% of loss of conductivity occurs.

$$\Psi_{\mathrm{air}} = \frac{2}{a} + b$$

where $\Psi_{\mathrm{air}}$ is the air entry point, an estimate of xylem tension (MPa) when cavitation starts.

$$\Psi_{\max} = -\frac{2}{a} + b$$

where $\Psi_{\max}$ is the full embolism point, an estimate of the maximum tension (MPa) in the xylem before failing and becoming non-conductive.

$$s = 25 \cdot a$$

where $s$ is the slope of the linear portion of the VC curve (% loss of $k$ MPa$^{-1}$), an estimate of rate of change in loss of $k$ per unit change in xylem tension.

Table 1. Least square means of diameter at breast height (DBH), total height, total stem volume without bark (Volume), leaf area ($L_A$) and all-sided specific leaf area (SLA) for longleaf and slash pines.

| Trait | Unit | Species | | $P > F^*$ species |
|---|---|---|---|---|
| | | Longleaf | Slash | |
| DBH | (mm) | 326.1 | 348.5 | 0.664 |
| Height | (m) | 24.51 | 26.67 | 0.161 |
| Volume | ($m^3$) | 0.91 | 1.21 | 0.545 |
| $L_A$ | ($m^2$) | 61.22 | 104.84 | 0.127 |
| SLA | ($cm^2\ g^{-1}$) | 96.29 | 98.06 | 0.812 |

*$P$-values using mixed model procedure ($n$ = 7 for DBH and height; $n$ = 4 for all other variables).

### *Leaf to sapwood area ratio*

At the end of the study, all four trees per species selected for leaf water potential, sapflow, hydraulic conductivity (on trunk, roots and branches) and leaf area measurements were felled to determine total tree leaf area ($L_A$, $m^2$), using a destructive determination of leaf mass ($L_W$, g) in conjunction with tree-specific estimations of all-sided specific leaf area (SLA, $cm^2\ g^{-1}$). Trees were felled at a stump height of ~0.2 m and all branches were cut at the point where live needles started. All foliated branch tips were weighed green in the field and summed to determine whole-tree branch tip fresh mass. For each tree, 20 randomly selected subsamples of branch tips were weighed, bagged and brought back to the laboratory for separate measurement of moisture content and dry masses of wood and needles of each branch tip. Dry mass of all living needles of the whole-tree crown ($L_W$) was calculated as the product of field-determined whole-tree branch tip fresh mass and the average dry needle to fresh branch tip ratios derived from the 20 branch tip subsamples. Needles were weighed separately into two age classes, current year and older needles, so dry needle to fresh branch tip ratios were also separately calculated for each needle type.

SLA was determined as the ratio between surface area and dry weight of needles for each needle age class. Individual needle surface area was calculated according to Murthy and Dougherty (1997) and Niinemets et al. (2001) from needle radius and length measured with a 10× scaled magnifier and a digital caliper (CD-6, Mitutoyo, Kawasaki, Japan), respectively, on 10 needles per tree. After surface area determination, the needles were oven-dried for 48 h at 75 °C and weighed to the nearest 0.0001 g (XA-100, Denver Instruments). A weighted average SLA (Table 1) was determined for each tree after including the proportion of leaf mass of each needle age. To determine daily $L_A$ for each tree, seasonal patterns were developed using information previously collected from periodic measurements of leaf area index from January 2000 to January 2006 (Powell et al. 2008). $L_A$ was estimated backward in time from $L_A$ measurement day (between 21 June and 9 July) until sapflow installation day (17 April).

In all measured trees, at the same point where sapflow probes were installed, sapwood area ($S_A$, $m^2$) was estimated at the end of the study by directly measuring sapwood depth and stem di-

ameter in 20-cm-thick disks extracted after the trees were felled for foliar biomass and leaf area determination at the point where sapflow probes were installed (at 1.8 m and crown-base heights). The disks were transported back to the laboratory covered with wet towels in plastic bags and stored at 5 °C for further hydraulic conductivity measurements. Aboveground sapwood volume below crown base was calculated for each tree by using sapwood area measured at stump and crown base and distance from stump to crown base. Stem diameter and bark thickness were measured each 2 m to determine stem volume. After determination of $L_A$ and sapwood area ($S_A$, $m^2$) at $S_{base}$ or $S_{crown}$, Huber value (HV, or sapwood to leaf area ratio, $m^2\ m^{-2} \times 10^{-4}$) was calculated for each tree as $S_A$ at $S_{base}$ or $S_{crown}$, divided by total $L_A$. In the case of branches, HV was computed as sapwood area of the segment (determined for $k$ measurements) divided by branch leaf area distal to the segment.

### *Tracheid length, diameter and cell-wall thickness*

Tracheid diameter, lumen diameter, double cell-wall thickness and length were measured in all segments used for the VC curves. For tracheid lumen diameter and double cell-wall thickness estimations, cross sections made with a vibratome (Leica VT1000 S; Leica Microsystems, Wetzlar, Germany) of ~50 µm thickness were extracted from a plane ~1 cm away from the proximal end of each sample and mounted in deionized distilled water over microscope slides. Using a digital camera (Retiga 1300; QIMAGING, Surrey, BC, Canada) attached to a light microscope (Olympus Ix70; Olympus, Tokyo, Japan), images of the xylem were captured with image capture software (QCapture Suite V2.60, QIMAGING) with a magnification of 20× for roots and 40× for trunk and branch samples. Ten to 15 images were randomly selected across the radial distribution of the whole cross section. A minimum of 400 tracheids were measured on each sample.

Conduit lumen area and perimeter of all tracheids contained in each image were measured, encompassing both latewood and earlywood using image analysis software (Image-Pro Plus 4.0, Media Cybernetics, Bethesda, MD, USA). Double cell-wall thickness ($t$, µm) was directly measured in 20 pairs of cells on all images using the same image analysis software; cell-wall thickness (cwt, µm) was computed as double cell-wall thickness divided by two. Using tracheid lumen area and perimeter measurements, and assuming an elliptical shape for all conduits, major (a) and minor (b) semi-axes for the ellipse equivalent were solved for each tracheid. Equivalent diameter (d) for elliptical conduit was calculated using the formula given by White (1991):

$$d = \left(\frac{32\cdot(a\cdot b)^3}{a^2+b^2}\right)^{1/4}$$

where $a$ and $b$ are major and minor semi-axes for the ellipse equivalent. For each image, mean total tracheid major and minor semi-axes ($a'$ and $b'$, respectively) were computed as average $a$ and $b$ plus average cwt, respectively. Mean tracheid area ($a_{tr}$, $m^2$) was computed as $a_{tr} = \pi\cdot a'\cdot b'$. The average number of tracheids per unit area ($T_n$, $m^{-2}$) was computed as $T_n = a_{tr}^{-1}$. The mean hydraulic diameter ($D_h$, µm) was calculated according to Tyree and Zimmermann (2002) as:

$$D_h = \left(\frac{\sum d^4}{N}\right)^{1/4}$$

where $N$ is the total number of conduits measured for each sample after pooling all 10–15 images per cross section. Single cell wall to span ratio ($C$) was calculated as cwt divided by $D_h$. In order to estimate a conduit implosion resistance index, cell-wall strength factor was calculated for each segment by using the double wall thickness/span ratio $(t/D_h)^2$ (Hacke et al. 2001). Using $D_h$ in the Hagen–Poiseuille equation, an estimate of theoretical whole-wood lumen specific conductivity ($k_{s\text{-lumen}}$, kg $s^{-1}$ $MPa^{-1}$ $m^{-1}$) was determined according to Domec et al. (2006):

$$k_{s\text{-lumen}} = \frac{T_n\cdot\pi\cdot D_h^4}{128\cdot\eta}$$

where $T_n$ is the average number of tracheids per unit area ($m^{-2}$) and $\eta$ is the viscosity of water at 25 °C ($8.9 \times 10^{-10}$ MPa s). $k_{s\text{-lumen}}$ value was converted to the same units as $k_s$ (kg $s^{-1}$ $MPa^{-1}$ $m^{-1}$) by multiplying by water density, which equals 1000 kg $m^{-3}$ $H_2O$. Whole-wood specific conductivity of the pits ($k_{s\text{-pit}}$, kg $s^{-1}$ $MPa^{-1}$ $m^{-1}$), which represents the parallel conductivity of all pits on a tissue basis, was computed as the difference between the inverse of sapwood-specific maximum conductivity (e.g., $k_{s\text{-max}}$) and $k_{s\text{-lumen}}$ following Domec et al. (2006), where $k_{s\text{-max}}$ represents the conductivities of pits and lumen together at full saturation:

$$k_{s\text{-pit}} = \left(\frac{1}{k_{s\text{-max}}} + \frac{1}{k_{s\text{-lumen}}}\right)^{-1}$$

Tracheid length was determined with a fiber quality analyzer (FQA; OpTest Equipment, Inc., Hawkesbury, ON, Canada) on previously macerated samples (Robertson et al. 1999). Twenty-millimeter longitudinal strips made with a razor blade were placed in 10-ml glass containers. A maceration procedure using acetic acid and peroxide was performed following the Ruzin (1999) protocol. After maceration, the samples were washed with deionized water and left overnight in water, then transferred to 50% ethanol and sent to the Wood and Fiber Quality Laboratory at the University of British Columbia, Canada, for FQA analysis. As tracheid length distribution is biased towards shorter tracheids, an estimate of tracheid length, the length-weighted tracheid length ($L_t$, mm), was calculated as:

$$L_t = \frac{\sum(n_i\cdot l_i^2)}{\sum(n_i\cdot l_i)}$$

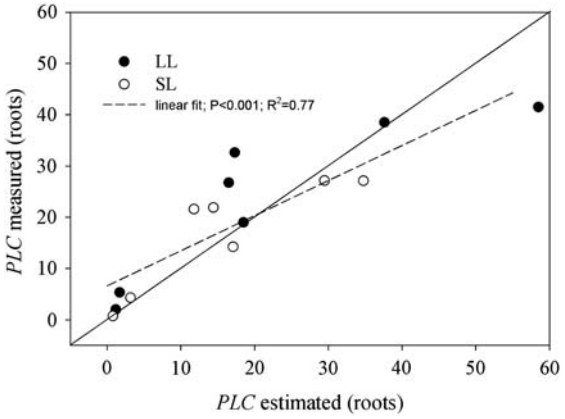


Figure 1. Estimated PLC using the relationship between water potential and loss of conductivity from VC curves versus measured PLC on roots of longleaf and slash pine trees. As samples were taken early in the morning, soil matric potential was used to estimate xylem water potential. The diagonal line represents a 1:1 relationship and the dashed line represents a linear fit.

where $l_i$ is the measured fiber length of the $i$th length class and $n_i$ is the number of tracheids measured of the $i$th length class (Schimleck et al. 2004).

### *Specific gravity*

On all samples that were hydraulically tested, 10-mm length sections were cut out and specific gravity (SG) was calculated as (Simpson 1993):

$$SG = \frac{W_d / V_g}{\rho_w}$$

where $W_d$ is the oven-dry weight of wood (g), $V_g$ is the volume of wood at moisture condition ($cm^3$) and $\rho_w$ is the density of water (1 g $cm^{-3}$). For $S_{base}$ and $S_{crown}$, $V_g$ was determined using X-ray computed tomography with a SCANCO Micro-CT 35 scanner (SCANCO Medical, Bassersdorf, Switzerland). For roots and branches, $V_g$ was determined using the water displacement method (Hacke et al. 2000*b*, Pittermann et al. 2006*b*). On each sample of roots and branches, the pith and the bark were removed with a razor blade. After $V_g$ determination, the sections were oven-dried at 60 °C for 3 days and $W_d$ was determined.

### *Statistical analysis*

Analysis of variance was used to analyze effects of organ and species in $k$, vulnerability to cavitation and tracheid size, including Bonferroni adjustments for differences in least square means (PROC MIXED, SAS Inc., Cary, NC, USA). The linear model for the analysis was:

$$Y_{ijk} = \mu + S_i + t_{k(i)} + O_{j(i)} + \varepsilon_{ijk}$$

where $Y_{ijk}$ is the parameter value of the $j^{th}$ organ nested in the $i^{th}$ species in the $k^{th}$ tree; $i$ = LL and SL; $j$ = root, $S_{base}$, $S_{crown}$ and branch; $k$ = 1, 2, 3 and 4 for trees (replications); and

$\mu$ = population mean,
$S_i$ = fixed effect of species (LL or SL),
$t_{k(i)}$ = random effect of tree nested within species,
$O_{j(i)}$ = fixed effect of organ (root, $S_{base}$, $S_{crown}$ and branch) nested within species,
$\varepsilon_{ijk}$ = error term ~NID (0, $\sigma^2_\varepsilon$) (NID, normally and independently distributed)

For roots and branches, $k$ = 1, 2, 3, 4, 5, 6 and 7.

The radial profile in hydraulic conductivity was analyzed after normalizing axial distance of the cambium relative to sapwood thickness for each tree (divided into classes of 20% of sapwood thickness) and using repeated measures analysis including Bonferroni adjustments for differences in least square means (Littell et al. 2006).

## Results

### *Hydraulic conductivity and vulnerability to cavitation*

As sampling was carried out on different days with variable soil moisture conditions ($\Psi_s$ at 0.5 m depth varied between −0.05 and −1.51 MPa on LL), native PLC could not be compared between organs or species. However, early in the morning, when root sampling was done, it is reasonable that $\Psi_s$ can be used as a proxy of root water potential. A good agreement was observed between PLC determined with measurements of $k_{s\text{-}nat}$ and $k_{s\text{-}max}$ and the estimation obtained with VC curves using $\Psi_s$ as root water potential ($P < 0.001$, $R^2 = 0.77$); the slope of this relationship was 0.99 when the intercept was forced through zero (Figure 1). In general, a low PLC (between 0 and 5%) was obtained on days with wet soil ($\Psi_s$ ~−0.1 MPa), and a high PLC (between 20 and 57%) was obtained on days with dry soil ($\Psi_s$ between −0.7 and −1.5 MPa). These results confirm the robustness of this relationship and provide a solid base for our analysis and discussion.

Native sapwood-specific hydraulic conductivity ($k_{s\text{-}nat}$) was not significantly different between LL and SL for any organ evaluated (Table 2). For LL, $k_{s\text{-}nat}$ was the same for roots and stem at the crown base ($S_{crown}$), and these differed from stem at 1.8 m height ($S_{base}$) and branches. No differences in $k_{s\text{-}nat}$ between root and $S_{crown}$ were observed. For SL, there was no difference in $k_{s\text{-}nat}$ among roots, $S_{base}$ and $S_{crown}$, but branches, on the other hand, had significantly lower $k_{s\text{-}nat}$ than the other organs.

After removing embolism by vacuum soaking, $k_{s\text{-}nat}$ increased between 7 and 24%, obtaining mean weighted values of maximum sapwood-specific hydraulic conductivity ($k_{s\text{-}max}$) for roots, $S_{base}$, $S_{crown}$ and branches, of 11.86, 6.81, 9.29 and 2.31 kg $s^{-1}$ $MPa^{-1}$ $m^{-1}$, respectively, for LL. Corresponding values for SL were 7.92, 7.69, 10.94 and 1.70 kg $s^{-1}$ $MPa^{-1}$ $m^{-1}$, respectively. SL and LL differed in $k_{s\text{-}max}$ for roots ($P = 0.02$). Thus, between-species $k_{s\text{-}max}$ significantly

Table 2. Least square means of hydraulic and tracheid anatomy traits evaluated for roots, stem bole at 1.8 m height ($S_{base}$), stem bole at crown base ($S_{crown}$) and branches for longleaf and slash pine trees. $k_{s\text{-}nat}$ is native stem-specific hydraulic conductivity (kg $s^{-1}MPa^{-1}$ $m^{-1}$); $k_{s\text{-}max}$ is maximum stem-specific hydraulic conductivity (kg $s^{-1}$ $MPa^{-1}$ $m^{-1}$); $k_{l\text{-}max}$ is maximum leaf-specific hydraulic conductivity (kg $s^{-1}$ $MPa^{-1}$ $m^{-1}$ × $10^{-4}$); $S_A$ is sapwood area ($m^2$); HV is sapwood to leaf area ratio ($m^2$ $m^{-2}$ × $10^{-4}$); ST is sapwood thickness (mm); $k$ is hydraulic conductivity (kg $s^{-1}$ $MPa^{-1}$ $m^{-1}$), $\Psi_{50}$ is the xylem tension at which 50% of loss of conductivity occurs (MPa); $s$ is the slope of the linear portion of the VC curve (% loss of $k$ $MPa^{-1}$); $\Psi_{air}$ is the air entry point (MPa); $\Psi_{max}$ is the full embolism point (MPa); SG is wood specific gravity; $L_t$ is tracheid length (mm); $D_h$ is tracheid mean hydraulic diameter (μm), cwt is the cell-wall thickness (μm); $C$ is the cell wall to lumen ratio; $(t/D_h)^2$ is the cell wall strength factor; $T_n$ is the average number of tracheids per unit area ($m^{-2}$); $k_{s\text{-}lumen}$ is the theoretical whole-wood lumen specific conductivity (kg $s^{-1}$ $MPa^{-1}$ $m^{-1}$); $k_{s\text{-}pit}$ is the whole-wood specific conductivity of the pits (kg $s^{-1}$ $MPa^{-1}$ $m^{-1}$).

| Trait | Tissue | Species | | | | $P > F^*$ species |
|---|---|---|---|---|---|---|
| | | Longleaf | | Slash | | |
| $k_{s\text{-}nat}$ | Root | 10.39 | a | 7.25 | a | 0.257 |
| | $S_{base}$ | 5.12 | b | 6.87 | a | 0.099 |
| | $S_{crown}$ | 8.61 | a | 10.36 | a | 0.415 |
| | Branch | 2.11 | c | 1.49 | c | 0.251 |
| $k_{s\text{-}max}$ | Root | 11.86 | a | 7.92 | a | 0.023 |
| | $S_{base}$ | 6.81 | b | 7.69 | a | 0.178 |
| | $S_{crown}$ | 9.29 | b | 10.94 | a | 0.422 |
| | Branch | 2.31 | c | 1.70 | c | 0.322 |
| $k_{l\text{-}max}$ | $S_{base}$ | 5.61 | b | 4.084 | b | 0.464 |
| | $S_{crown}$ | 3.56 | b | 2.884 | b | 0.244 |
| | Branch | 0.210 | a | 0.242 | a | 0.713 |
| $S_A$ | $S_{base}$ | 0.040 | a | 0.052 | a | 0.438 |
| | $S_{crown}$ | 0.020 | b | 0.027 | b | 0.474 |
| HV | $S_{base}$ | 8.25 | a | 5.15 | a | 0.086 |
| | $S_{crown}$ | 3.86 | b | 2.89 | b | 0.189 |
| | Branch | 1.35 | b | 1.77 | b | 0.624 |
| ST | $S_{base}$ | 52.1 | a | 69.3 | a | 0.078 |
| | $S_{crown}$ | 56.1 | a | 58.6 | b | 0.822 |
| $k$ | $S_{base}$ | 0.26 | a | 0.41 | a | 0.297 |
| | $S_{crown}$ | 0.19 | a | 0.32 | a | 0.330 |
| $\Psi_{50}$ | Root | −1.31 | b | −1.33 | b | 0.878 |
| | $S_{base}$ | −1.35 | ab | −1.16 | ab | 0.111 |
| | $S_{crown}$ | −1.47 | ab | −1.52 | ab | 0.718 |
| | Branch | −1.81 | a | −1.74 | a | 0.758 |
| $s$ | Root | 87.66 | b | 96.9 | b | 0.262 |
| | $S_{base}$ | 61.61 | b | 60.75 | ab | 0.998 |
| | $S_{crown}$ | 67.31 | b | 74.93 | ab | 0.606 |
| | Branch | 41.73 | a | 51.84 | a | 0.115 |
| $\Psi_{air}$ | Root | −0.69 | a | −0.69 | a | 0.721 |
| | $S_{base}$ | −0.52 | a | −0.32 | b | 0.074 |
| | $S_{crown}$ | −0.72 | a | −0.82 | a | 0.537 |
| | Branch | −0.55 | a | −0.72 | ab | 0.393 |
| $\Psi_{max}$ | Root | −1.96 | b | −1.95 | b | 0.944 |
| | $S_{base}$ | −2.18 | b | −1.99 | b | 0.217 |
| | $S_{crown}$ | −2.22 | b | −2.22 | b | 0.366 |
| | Branch | −3.04 | a | −2.75 | a | 0.984 |
| SG | Root | 0.209 | c | 0.228 | c | 0.728 |
| | $S_{base}$ | 0.587 | b | 0.580 | b | 0.858 |
| | $S_{crown}$ | 0.506 | a | 0.498 | a | 0.747 |
| | Branch | 0.431 | a | 0.429 | a | 0.909 |
| $L_t$ | Root | 2.61 | a | 2.44 | a | 0.448 |
| | $S_{base}$ | 1.33 | b | 1.37 | b | 0.230 |
| | $S_{crown}$ | 2.24 | a | 2.20 | a | 0.848 |
| | Branch | 1.11 | b | 1.16 | b | 0.374 |
| $D_h$ | Root | 37.42 | a | 32.81 | a | 0.238 |
| | $S_{base}$ | 28.37 | b | 28.72 | a | 0.656 |
| | $S_{crown}$ | 26.78 | b | 31.60 | a | 0.047 |
| | Branch | 14.14 | c | 13.66 | b | 0.689 |
| cwt | Root | 3.83 | b | 2.77 | b | 0.014 |
| | $S_{base}$ | 5.75 | a | 6.19 | a | 0.470 |
| | $S_{crown}$ | 5.73 | a | 5.89 | a | 0.822 |
| | Branch | 2.41 | c | 2.49 | b | 0.536 |
| $C$ | Root | 0.105 | a | 0.093 | a | 0.194 |
| | $S_{base}$ | 0.207 | b | 0.217 | b | 0.173 |
| | $S_{crown}$ | 0.214 | b | 0.186 | b | 0.151 |
| | Branch | 0.176 | b | 0.184 | b | 0.640 |
| $(t/D_h)^2$ | Root | 0.0459 | a | 0.0322 | a | 0.094 |
| | $S_{base}$ | 0.1739 | b | 0.1908 | b | 0.657 |
| | $S_{crown}$ | 0.1840 | b | 0.1397 | b | 0.153 |
| | Branch | 0.1292 | b | 0.1368 | b | 0.754 |
| $T_n$ | Root | 905 | b | 1285 | b | 0.047 |
| | $S_{base}$ | 1153 | b | 1029 | b | 0.665 |
| | $S_{crown}$ | 1208 | b | 916 | b | 0.274 |
| | Branch | 4224 | a | 4048 | a | 0.714 |
| $k_{s\text{-}lumen}$ | Root | 44.08 | a | 34.84 | a | 0.018 |
| | $S_{base}$ | 16.15 | b | 17.14 | b | 0.758 |
| | $S_{crown}$ | 14.83 | b | 22.59 | ab | 0.093 |
| | Branch | 4.39 | c | 3.47 | c | 0.430 |
| $k_{s\text{-}pit}$ | Root | 18.70 | ab | 11.05 | ab | 0.037 |
| | $S_{base}$ | 9.40 | b | 12.87 | ab | 0.825 |
| | $S_{crown}$ | 25.14 | a | 28.13 | a | 0.623 |
| | Branch | 5.71 | b | 4.89 | b | 0.765 |

Significant differences ($P < 0.05$) in parameters between organs are indicated by different letters. *$P$-values using mixed model procedure ($n = 7$ for roots and branches; $n = 4$ for $S_{base}$ and $S_{crown}$).

differed only in roots. Leaf-specific maximum hydraulic conductivity ($k_{l\text{-}max}$) was not different between species for any organ evaluated (Table 2). Within species, $k_{l\text{-}max}$ of branches was lower than $S_{base}$ and $S_{crown}$.

For both species, branches were less vulnerable to cavitation than roots ($\Psi_{50}$ = −1.77 and −1.32 MPa, respectively) but did not differ between $S_{base}$ and $S_{crown}$ (Figure 2; Table 2). A species contrast showed no difference in $\Psi_{50}$ for any organ tested ($P > 0.11$; Table 2). The slope of the linear portion of the VC curve ($s$) is an index of the sensitivity of $k_s$ to changes in xylem water potential (Domec and Gartner 2001): the higher $s$, the greater the reduction in $k_s$ (PLC) per unit reduction in xylem water potential. No differences in $s$ between species were found across all organs ($P > 0.07$; Table 2). However, in LL, $s$ of branches was smaller than root and

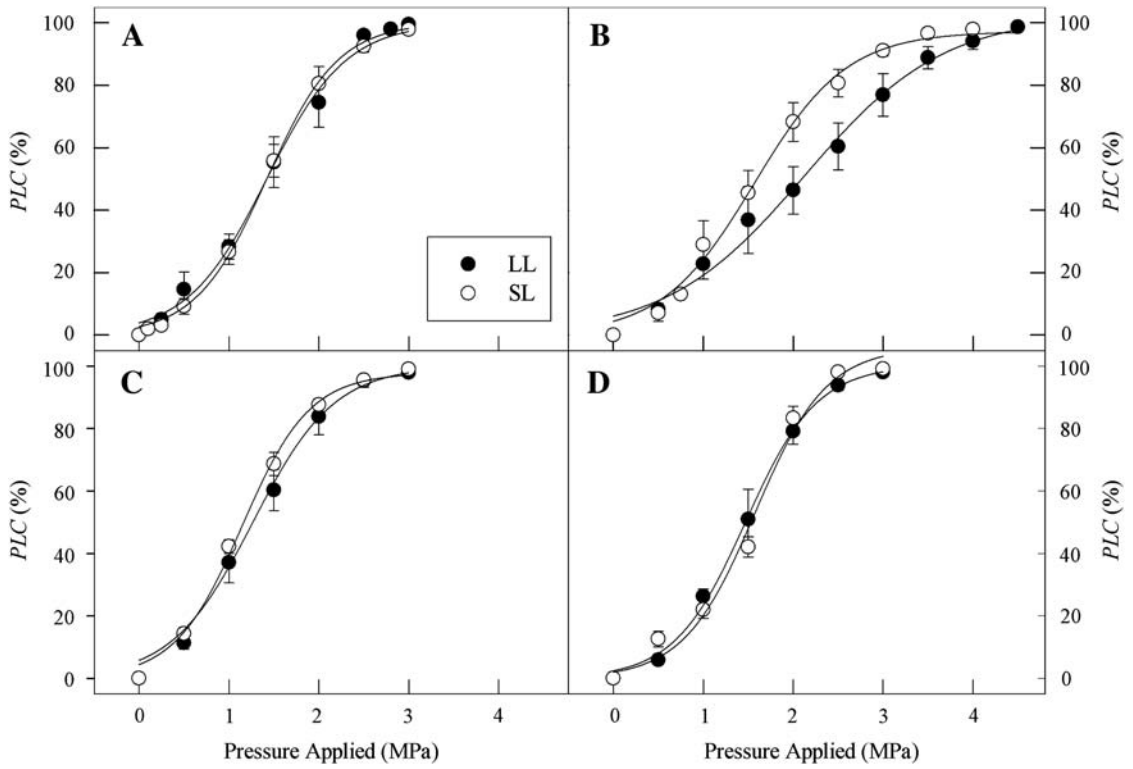


Figure 2. Percentage loss of conductivity (PLC) versus the applied air pressure in longleaf pine (filled circle) and slash pine (open circle) (mean ± SE) for roots (A; $n$ = 7), branches (B; $n$ = 7), stem at 1.8 m (C; $n$ = 4) and stem at crown base (D; $n$ = 4).

trunk xylem. In contrast, SL only showed differences in $s$ between roots and branches (Table 2). The air entry point ($\Psi_{air}$) and the xylem water potential causing full embolism ($\Psi_{max}$) were not different between species for any organ measured. In general, $\Psi_{max}$ of branches was significantly more negative than $S_{base}$, $S_{crown}$ and roots. In LL, $\Psi_{air}$ was not different across organs, but for SL, $\Psi_{air}$ of $S_{base}$ was higher than $S_{crown}$ and roots (Table 2).

When all organs were pooled, there was a significant but weak relationship between $k_{s\text{-}max}$ and $\Psi_{50}$ ($P$ = 0.009, $R^2$ = 0.16; Figure 3), indicating a weak trade-off between water conduction efficiency and safety.

### *Radial profile in hydraulic conductivity*

There were no differences in $k_{s\text{-}nat}$ or $k_{s\text{-}max}$ along the sapwood radius for either species, even though at $S_{base}$ $k_{s\text{-}max}$ increased 18 and 24% from the outer 20% to the outer 20–40% of sapwood thickness for LL and SL, respectively (Figure 4). Close to the inner fringe of sapwood, at 80–100% of the thickness, average $k_{s\text{-}max}$ was 6.55 and 6.76 kg $s^{-1}$ $MPa^{-1}$ $m^{-1}$, for LL and SL, respectively, corresponding to a 9.9 and 2.4% reduction in $k_{s\text{-}max}$ compared with outermost rings (Figure 4A). At the crown base, $k_{s\text{-}max}$ of LL and SL averaged 8.75, 10.69 and 7.41, and 12.40, 12.37 and 11.68 kg $s^{-1}$ $MPa^{-1}$ $m^{-1}$at 0–20%, 40–60% and 80–100% of sapwood thickness, respectively. Within each species, there were no statistical differences in $k_{s\text{-}max}$ along the sapwood radius.

### *Tracheid anatomy*

There were no differences between species in weighted tracheid length ($L_t$) for any tissue evaluated (Table 2). Average $L_t$ for roots, $S_{crown}$, $S_{base}$ and branches were 2.61, 2.24, 1.33 and 1.11 mm for LL; and 2.44, 2.20, 1.37 and 1.16 mm for SL, respectively. For both species, there were no differences in $L_t$ between roots and $S_{crown}$, and between $S_{base}$ and branches; roots and $S_{crown}$ $L_t$ was statistically larger than the $S_{base}$ and branches.

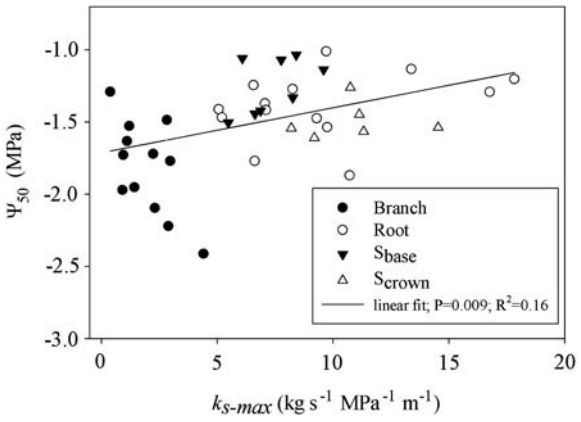


Figure 3. Xylem tension that causes 50% of loss of conductivity ($\Psi_{50}$) versus maximum sapwood-specific hydraulic conductivity ($k_{s\text{-}max}$) for branch, root, $S_{base}$ and $S_{crown}$. Both species are included.

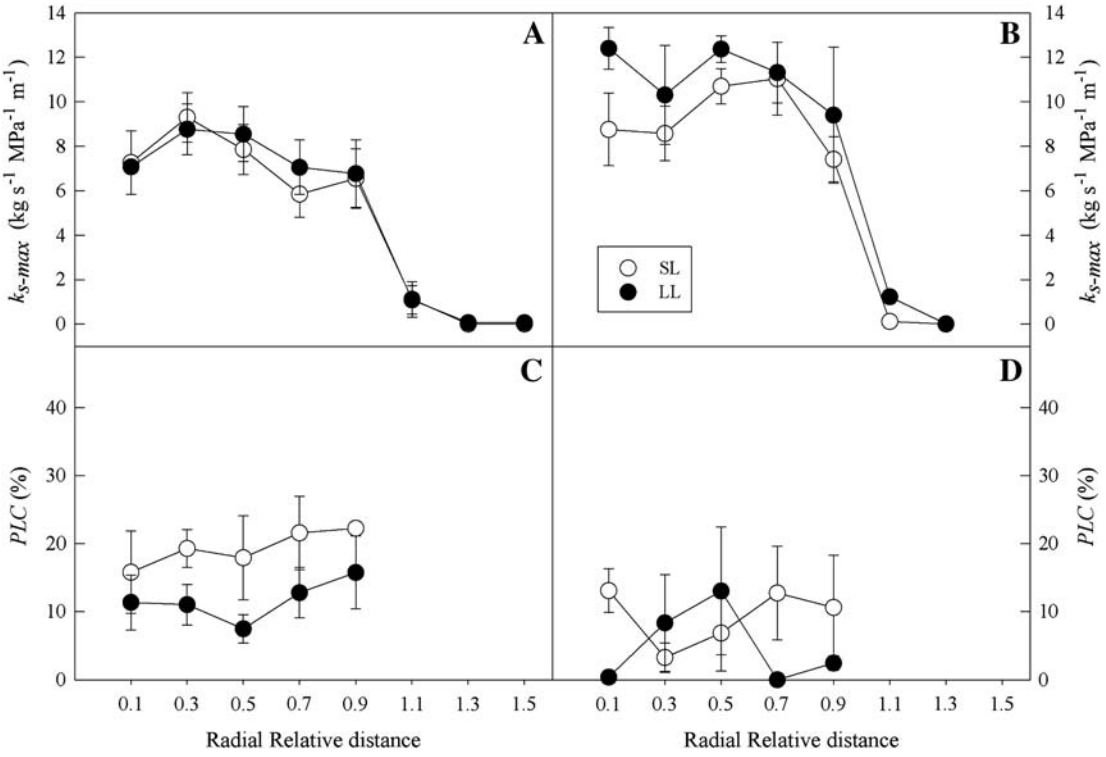


Figure 4. Radial profile in maximum sapwood-specific hydraulic conductivity ($k_{s\text{-}max}$; A, B) and percentage loss of conductivity (PLC; C, D) for stem at 1.8 m height (A, C) and at crown base (B, D) for longleaf and slash pine. Relative radial distance is defined as the distance from bark to measurement point divided by distance from bark to sapwood/heartwood boundary.

Tracheid hydraulic diameter ($D_h$) was not different between species for roots, $S_{base}$ and branches ($P$ = 0.112, 0.845 and 0.689, respectively) but was slightly larger for SL at the $S_{crown}$ ($P$ = 0.047). Average $D_h$ for roots, $S_{crown}$, $S_{base}$ and branches were 37.4 and 32.8, 28.4 and 27.8, 26.8 and 31.6, and 14.1 and 13.7 μm for LL and SL, respectively (Table 2).

Regressions with $k_{s\text{-}max}$ and $\Psi_{50}$ against $L_t$ and $D_h$ were not different between species ($P > 0.38$), thus they were pooled (Figure 5). In the combined data, significant positive correlations for $L_t$ and $D_h$ with $k_{s\text{-}max}$ ($P < 0.001$) were found and variation in $L_t$ and $D_h$ accounted, separately, for 46% and 73% of this variation. While $D_h$ was linearly correlated with $k_{s\text{-}max}$ (Figure 5B), $L_t$ was non-linearly correlated with $k_{s\text{-}max}$, independent of the organ and species tested (Figure 5A). For $L_t$ smaller than ~1.5–2.0 mm, resistance to cavitation sharply increased as $L_t$ decreased; beyond that threshold value, $\Psi_{50}$ was relatively constant around −1.0 to −1.5 MPa independent of the organ and species tested, not being related to increases in $L_t$ (Table 5C). When all organs were considered, there was a significant ($P < 0.001$) but weak ($R^2$ = 0.29) relationship between $D_h$ and $\Psi_{50}$, but within roots, $S_{crown}$, $S_{base}$ and branches, there was no relationship between $D_h$ and $\Psi_{50}$. When all organs were considered, there was a positive correlation between $L_t$ and $D_h$ ($P < 0.001$, $R^2$ = 0.45; Figure 6B), but if branches were not included, there was no relationship between $L_t$ and $D_h$ ($P$ = 0.29, $R^2$ = 0.04) for tracheids in branches, $S_{base}$ and $S_{crown}$.

Between species, cwt was only different for roots ($P <$ 0.001), averaging 3.83 and 2.77 μm for LL and SL, respectively. For both species, tracheid cell walls were thicker at $S_{base}$ and $S_{crown}$ than in roots and branches, with cwt of roots also larger than branches on LL (Table 2). There were no significant differences between species in $C$ for any tissue evaluated, averaging 0.09, 0.18, 0.21 and 0.20 for roots, branches, $S_{base}$ and $S_{crown}$, respectively. For tracheids of similar $D_h$ (averaging ~30 μm in Figure 6A), root xylem cells were much less reinforced (smaller $C$) than $S_{base}$ and $S_{crown}$. On the other hand, branch tracheids were more reinforced than roots, but a reduction in diameter of branch tracheids, for similar cwt compared with roots, was the cause of the difference in $C$ (Figure 6A).

Cell-wall strength, $(t/D_h)^2$, was not different between species for any organ evaluated (Table 2). Average $(t/D_h)^2$ for roots, $S_{crown}$, $S_{base}$ and branches was 0.040, 0.183, 0.162 and 0.133, respectively. There were no differences in $(t/D_h)^2$ between $S_{crown}$, $S_{base}$ and branches, but $(t/D_h)^2$ of roots was statistically lower than the other organs. Across species and organs, there was a strong relationship between $(t/D_h)^2$ and SG ($P < 0.001$; $R^2$ = 0.635; data not shown) but no relationship between $(t/D_h)^2$ and $k_{s\text{-}max}$ ($P$ = 0.47) or $\Psi_{50}$ ($P$ = 0.09).

The number of tracheids per unit area ($T_n$) was not different between species for branches, $S_{base}$ and $S_{crown}$ but was different for roots ($P$ = 0.046, Table 2). Average $T_n$ was significantly higher in branches than the other tissues, averaging

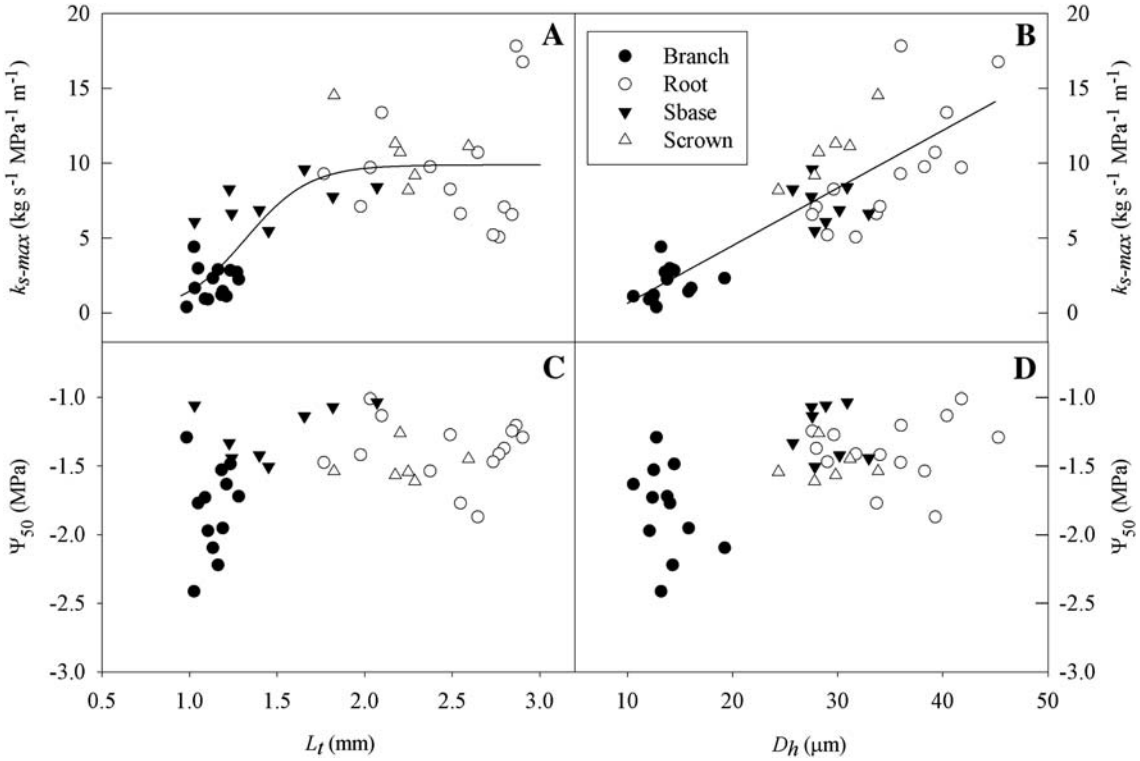


Figure 5. Maximum sapwood-specific hydraulic conductivity ($k_{s\text{-}max}$; A, B) and xylem tension that causes 50% of loss of conductivity ($\Psi_{50}$; C, D) versus tracheid length ($L_t$; A, C) and hydraulic tracheid lumen diameter ($D_h$; B, D) for longleaf and slash pine trees pooled. All organs measured (root, $S_{base}$, $S_{crown}$ and branch) are included.

4136, 1095, 1091 and 1061 tracheids per square millimeter for branches, roots, $S_{base}$ and $S_{crown}$, respectively.

To estimate the impact of each tracheid anatomy trait measured on $k_{s\text{-}max}$ and $\Psi_{50}$, multiple linear regressions were performed with cwt, $T_n$ and $C$ as well as $L_t$ and $D_h$ in the model. For $k_{s\text{-}max}$, $D_h$, $L_t$ and $C$ were all significant variables, accounting for 73.4, 2.4 and 1.6% of total $k_{s\text{-}max}$ variability (whole-model $R^2 = 0.77$). For $\Psi_{50}$, only $T_n$ was significant, accounting for 30.2% of total $\Psi_{50}$ variability. For the same $D_h$, tracheids in $S_{base}$ were shorter than tracheids at the $S_{crown}$ (Table 2; Figure 6B), and this difference in tracheid length (included as $D_h$ to $L_t$ ratio in covariance analysis) accounted for most of the variation in $k_{s\text{-}max}$ between $S_{base}$ and $S_{crown}$ ($P = 0.03$).

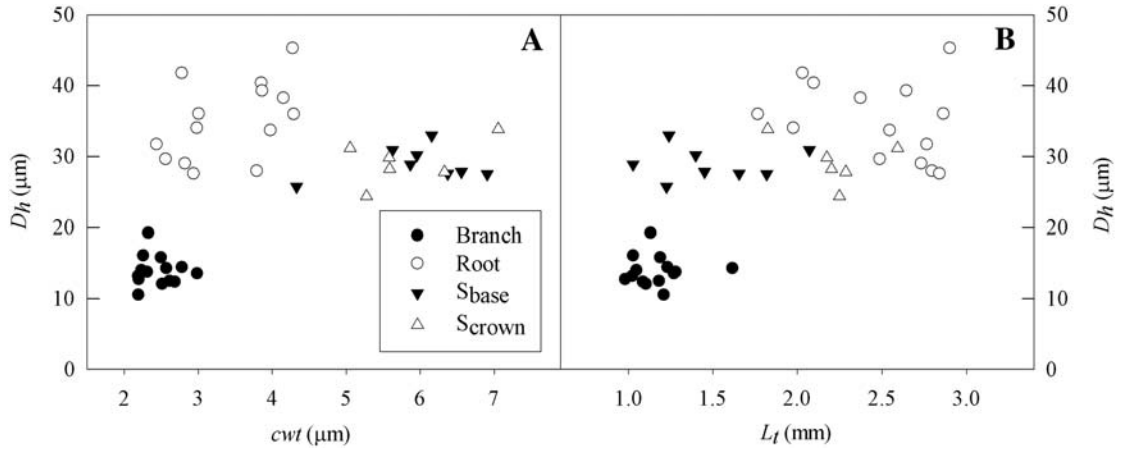


Figure 6. Allometry of tracheids of longleaf and slash pine trees. Relationship of mean hydraulic diameter ($D_h$) with cell-wall thickness (cwt; A) and tracheid length ($L_t$; B) for different organs evaluated. Both species are included.

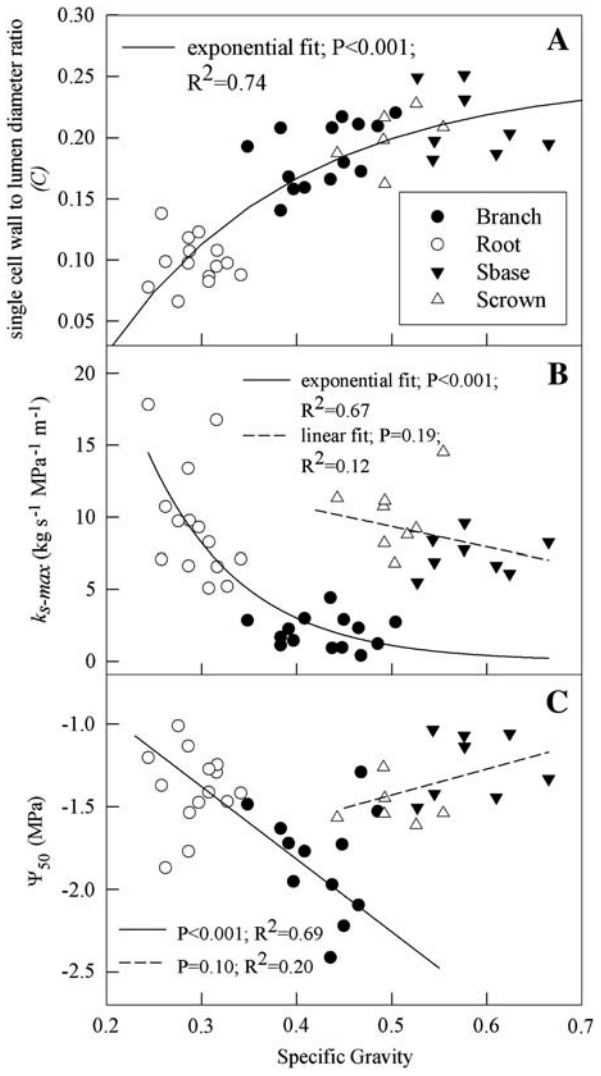


Figure 7. Relationships between specific gravity (SG) and (A) single cell wall to hydraulic diameter ratio ($C$), (B) maximum sapwood-specific hydraulic conductivity ($k_{s\text{-}max}$) and (C) vulnerability to cavitation ($\Psi_{50}$) for roots, branches, $S_{base}$ and $S_{crown}$ of longleaf and slash pine (see symbol legend on each figure).

### *Specific gravity*

Mean SG was not different between LL and SL for all organs evaluated (Table 2) but was different between organs within each species ($P < 0.001$ for both species). Across species, average SG for roots, branches, $S_{base}$ and $S_{crown}$ was 0.226, 0.429, 0.583 and 0.502, respectively. When all organs were pooled, SG was correlated with cell wall to hydraulic lumen diameter ratio ($C$), an exponential relationship that rises a maximum of $C \sim 0.25$ at SG $\sim 0.8$ was observed ($P < 0.001$; $R^2 = 0.74$; Figure 7A). When roots and branches were pooled after eliminating data of two outliers, SG was highly correlated with $k_{s\text{-}max}$ and $\Psi_{50}$ (Figure 7B and C) but not correlated with $S_{base}$ and $S_{crown}$ (note: the elimination of outliers does not affect the significance of the relationship but increased the correlation coefficient from 0.34 to 0.76, in the case of $\Psi_{50}$).

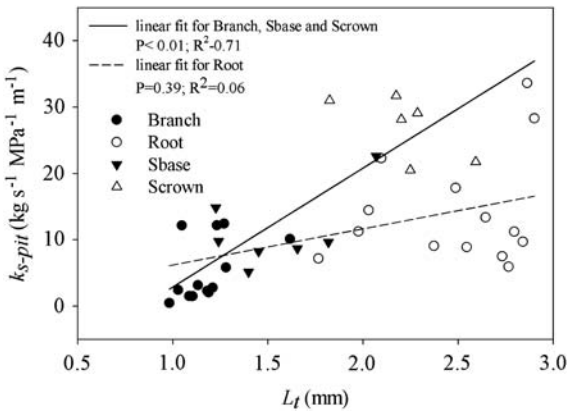


Figure 8. Relationship between tracheid length ($L_t$) and sapwood-specific hydraulic conductivity of pits ($k_{s\text{-}pit}$) for different organs evaluated in longleaf and slash pine trees. Lines represent linear fit for branches, $S_{base}$ and $S_{crown}$ (solid) and roots (dashed).

### *Pit and lumen conductivity*

There were no differences between species in $k_{s\text{-}lumen}$ or $k_{s\text{-}pit}$ for branches, $S_{base}$ and $S_{crown}$, but $k_{s\text{-}lumen}$ and $k_{s\text{-}pit}$ of roots were larger for LL ($P = 0.018$ and 0.037, respectively) (Table 2). For roots, pit resistance ($1/k_{s\text{-}pit}$) accounted for 72% of total hydraulic resistance, while for branches, $S_{base}$ and $S_{crown}$, pit resistance accounted for 53.7, 36.6 and 49.0% of the total resistance, respectively. Tracheid length was positively correlated with $k_{s\text{-}pit}$ when branches, $S_{base}$ and $S_{crown}$ were pooled ($P < 0.001$, $R^2 = 0.71$; Figure 8) but not for roots ($P = 0.39$). According to the Hagen–Poiseuille equation for capillaries, the relationship between $k_{s\text{-}max}$ and $k_{s\text{-}lumen}$ can be used as an index of the relative efficiency of water transport of the xylem in relation to the maximum theoretical conductivity. There was a significant and positive relationship between $k_{s\text{-}max}$ and the theoretical calculated $k_s$ (e.g., $k_{s\text{-}lumen}$); when all organs were pooled (Figure 9), the $k_{s\text{-}max}$ and $k_{s\text{-}lumen}$

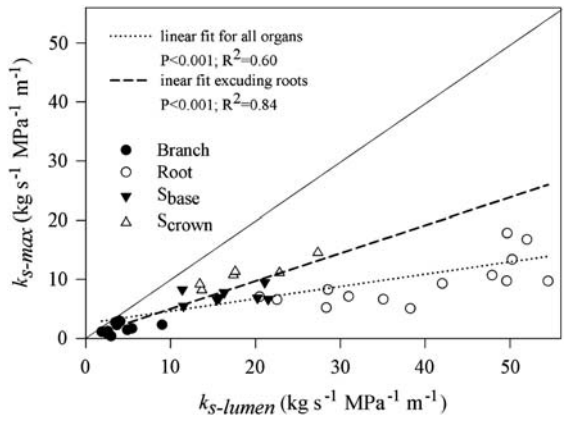


Figure 9. Maximum sapwood-specific hydraulic conductivity ($k_{s\text{-}max}$) versus sapwood-specific hydraulic conductivity of lumen ($k_{s\text{-}lumen}$) for branch, root, $S_{base}$ and $S_{crown}$. The solid diagonal line represents a 1:1 relationship and the dashed lines represent a linear fit. Both species are included.

ratio averaged 0.208. When roots were excluded from the analysis, the $R^2$ increased from 0.60 to 0.84, with a new slope of 0.471. Stem xylem of branches and $S_{crown}$ were the organs that deviated the least from the theoretical conductivity, averaging, across species, $k_{s\text{-}max}$ to $k_{s\text{-}lumen}$ ratio of 49.4 and 59.4%, respectively. Conversely, for $S_{base}$ and roots, this ratio was significantly lower than branches and the $S_{crown}$ ($P < 0.05$), averaging 36.5 and 25.5%, respectively. Between species, only roots were different in $k_{s\text{-}max}$ to $k_{s\text{-}lumen}$ ratio ($P = 0.019$), averaging 0.295 and 0.201 for LL and SL, respectively.

### *Huber value*

For LL, the ratio between $S_A$ and $L_A$ (HV) at $S_{base}$ was 2.1 and 6.1 times larger than HV at $S_{crown}$ and branches, respectively (Table 2). In the case of SL, HV at $S_{base}$ was 1.78 and 2.9 times larger than HV at $S_{crown}$ and branches. Even though there were no statistical differences between species ($P = 0.086$; Table 2), longleaf HV at $S_{base}$ and $S_{crown}$ was 60% and 33% larger than SL.

## Discussion

Trees are hydraulically complex organisms, exhibiting considerable within-organism variation in hydraulic conductivity and vulnerability to cavitation. Tree hydraulic traits have been shown to be associated with broad habitat preferences of widely variant species (e.g., Sperry et al. 1998), but to our knowledge have not been examined with regard to habitat preferences of co-occurring species. The goal of this study was to quantify within-organism variation in hydraulic traits in *P. palustris* and *P. elliottii* Engelm. var. *elliottii* to determine the tracheid morphological determinants of this variation and to link hydraulic traits to habitat preference for these co-occurring species.

Contrary to our first hypothesis, there were no differences in vulnerability to cavitation between slash and longleaf pine in any of the organs evaluated, but root $k_s$ of LL was significantly higher than SL, whereas branch and trunk $k_s$ did not differ between species. Tracheid allometry markedly changed between sapwood of roots, trunk and branches, possibly reflecting different mechanical constraints. Higher sapwood to leaf area ratio and higher maximum sapwood-specific hydraulic conductivity in roots of LL are anatomical traits that may provide LL with a competitive advantage on drier soil microsites.

Root xylem had higher water transport efficiency and was also the organ least resistant to cavitation (as compared with branches and trunk sapwood). Similar results with conifer species have been reported elsewhere (Kavanagh et al. 1999, Hacke et al. 2000*a*, 2000*b*, Martinez-Vilalta et al. 2002, Domec et al. 2006*b*, Maherali et al. 2006). Our mean values of $\Psi_{50}$ for roots were similar to those reported for *Pinus caribaea* M. and *Pinus taeda* L., closely related members of the subsection *Australes* of the *Pinus* genus that have been hybridized with longleaf and slash pine trees in breeding programs (Duncan et al. 1996). For *P. caribaea*, root $\Psi_{50}$ averaged −1.91 MPa (Pittermann et al. 2006*b*); for *P. taeda*, root average $\Psi_{50}$ ranged between −1.05 and −2.3 MPa (Hacke et al. 2000*a*) and −1.74 MPa (Maherali et al. 2006). The general trend that roots are more vulnerable to cavitation than shoots is associated with the fact that roots typically experience less negative water potentials.

It has been hypothesized that because roots tend to be more vulnerable to cavitation than other tree organs, they act as a hydraulic 'fuse' for the plant, limiting cavitation during soil drying to 'expendable' roots and protecting the aboveground parts of the hydraulic system (Sperry et al. 2002). Our data, when considered in the context of within-tree water potential gradients, do not support this hypothesis. In this study, the average difference in $\Psi_{50}$ between roots and $S_{crown}$ was −0.26 MPa, and the gravitational potential at the average crown height across species was −0.16 MPa ($P = 0.84$). Therefore, in real terms (subtracting gravitational potential), the difference in $\Psi_{50}$ between roots and $S_{crown}$ was only 0.1 MPa. When additional gradients due to hydraulic resistance are considered, the difference in $\Psi_{50}$ between roots and upper part of the trunk is compensatory and likely results in equal in situ risk of cavitation. In addition, it is important to consider that roots are not necessarily an 'expendable' organ. Most hydraulic conductivity studies in pines have been carried out with coarse roots (>2 mm diameter), and the construction cost of that lignified tissue in terms of carbon and energy, even though it is less than branches or trunk, is still high and directly correlated with loss of absorption of nutrients and water. Johnson et al. (2005) and Matamala et al. (2003) reported, for loblolly pine, that fine root mean life span was between 4.5 and 5.7 years, with even higher replacement time than for coarse roots. Therefore, loss of the absorbing surface due to xylem cavitation in roots is not a trivial cost for pine trees, and lateral roots (like those evaluated in this study) must be kept in place in order to ensure water and nutrient transport to the stem.

According to Hagen–Poiseuille, flow scales with the fourth power of conduit diameter, so as was expected, variations in $D_h$ had a much greater effect on $k_s$ than variations in $L_t$. The fact that $D_h$ and $L_t$ were correlated ($r = 0.67$) also explains the lack of influence of $L_t$ on total $k_s$ when the analysis was done across different organs. Nevertheless, for stem xylem, $k_{s\text{-}max}$ at $S_{crown}$ (20 m) was 39.5% higher than at $S_{base}$ (1.8 m), and the difference was correlated with the difference in $L_t$ ($D_h$ and cwt were not significantly different between $S_{base}$ and $S_{crown}$). Domec et al. (2005, 2006*a*) also reported that $k_s$ and $L_t$ were positively correlated in the trunk of *Pseudotsuga menziesii*. In this last study, the authors also reported a positive correlation between tracheid length and pit density as well as a negative correlation between tracheid diameter and pit chamber size. The positive relationship between $k_{s\text{-}pit}$ and $L_t$ (Figure 8) likely resulted because longer tracheids are wider and therefore have a greater total area of pit membrane connection, and larger tracheids are thought to have more porous pit membranes (Comstock 1970, Aumann and

Ford 2002). Furthermore, Comstock (1970) indicated that the number of pits transversed in series per unit length was inversely proportional to $L_t$, so the longer the tracheid, the fewer pits that have to be crossed as water moves longitudinally. Pit resistance in roots accounted for 72% of the total hydraulic resistance, while at the crown base pit resistance accounted for only 36.6%, even though $D_h$ and $L_t$ of roots were similar or greater than at $S_{crown}$ (Table 2). Differences in pit permeability, density and tracheid size distribution among roots, branches and stem may explain why roots showed no relationship with $k_{s\text{-}pit}$ Domec et al. (2006*a*) concluded that even though tracheid $D_h$ was correlated with $k_{s\text{-}pit}$, pit aperture and pit pore size were the tracheid structural characteristics that ultimately constrained hydraulic conductivity.

The relationship between $k_{s\text{-}max}$ and $\Psi_{50}$ indicated a significant but weak trade-off between water conduction efficiency and safety ($P = 0.009$, $R^2 = 0.16$; Figure 3). Several authors have reported similar results for gymnosperms; for example, Burgess and Pittermann (2006) for branches of *Sequoia sempervirens* and Maherali and De Lucia (2000) for branches of *Pinus ponderosa.* In contrast, Hacke et al. (2000*b*) reported no correlation between root tracheid diameter (directly correlated with $k_{s\text{-}max}$) and cavitation resistance. Conduit diameter was related to $k_s$ but was not necessarily important in determining $\Psi_{50}$ (Figure 5B and D) because the mechanism of water-stress-induced embolism (Tyree and Zimmermann 2002, Hacke et al. 2004, Domec et al. 2006) and embolism repair (Zwieniecki and Holbrook 2000) are more related to pit characteristics.

The relationship between SG, $k_{s\text{-}max}$ and $\Psi_{50}$ can be used to assess evidence of trade-offs between mechanical strength and water transport efficiency and safety. After pooling roots and branches, a negative exponential relationship ($P < 0.001$; $R^2 = 0.67$) was evident across roots and branches (circles in Figure 7B), similar to that reported across species (Santiago et al. 2004, Pittermann et al. 2006*a*, 2006*b*, Christensen-Dalsgaard et al. 2007). However, when trunk data were included (triangles in Figure 7), there was no relationship ($P = 0.35$), so it is reasonable to hypothesize that, due to high SG as well as $k_{s\text{-}max}$ in trunk tissue (Figure 7 and Table 2), higher pit conductance at $S_{crown}$ should compensate for increased wall area. Similar patterns emerged for the relationship between SG and $\Psi_{50}$; without trunk xylem, there was a strong linear relationship ($P < 0.001$; $R^2 = 0.69$), but after including trunk xylem there was no relationship ($P = 0.72$). For different conifer species, Sperry et al. (2006) also found a weak relationship between embolism resistance and wood density ($R^2 = 0.16$ for branches and 0.38 for roots).

Lateral root tracheids evolved with different mechanical constraints than tracheids of trunk or branches, and these appear to be reflected by differences in tracheid allometry. For example, SG and $C$ were almost 50% lower in roots than in branches or trunk tracheids (Table 2), with no difference between these two last organs. In contrast, branch tracheids had smaller cwt and $D_h$ values than trunk tracheids. The relationship between SG and $C$ (Figure 7A) reinforces this idea: branches, $S_{base}$ and $S_{crown}$ had different SG for similar $C$, indicating that differences in SG between these organs are related to differences in conduit size (and therefore to number of cells per unit area) rather than changes in mechanical reinforcement (Figure 7A). These differences in tracheid size were finally reflected in the number of cells per unit area, where branches had three to four times more cells per square millimeter than roots and trunk. These results suggest that when tracheid size is related to $k_s$ or $\Psi_{50}$ across organs, caution must be taken because results must depend on the organ evaluated.

Both longleaf and slash pines had similar mean values for most measured hydraulic traits. No differences in $k_{s\text{-}nat}$ or $\Psi_{50}$ were concordant with other water relation traits measured on the same trees, such as transpiration rate per unit leaf area, water storage use, stomatal regulation and whole-tree hydraulic conductance (Gonzalez-Benecke 2009). Nevertheless, root maximum sapwood-specific hydraulic conductivity was significantly larger in LL ($P = 0.023$; Table 2). This finding, associated with HV differences (although not statistically different at $S_{crown}$, longleaf HV was 60% larger than SL), may have important ecological implications associated with habitat characteristics of both species, where LL has the tendency to inhabit drier soil microsites than SL.

Differences in HV can be better assessed if we examine the model suggested by Whitehead et al. (1984), which combines the Penman–Monteith model and Darcy's Law, where stomatal (crown) conductance was directly proportional to $k_s$, $\Delta\Psi$ and HV, and inversely proportional to vapor pressure deficit and tree height: to maintain high stomatal conductance under water-stressed conditions, as low soil moisture, without the risk of excessive embolism by decreasing $\Psi$ (because vulnerability to embolism is similar between both species, Table 2), LL tends to produce roots with higher $k_s$ and at the same time allocate less carbon to foliage per unit $S_A$. This suite of traits is consistent with an adaptation to soil water deficits, because higher root $k_s$ allows LL to maintain high water supply to foliage at similar $\Delta\Psi$ (Table 2), and lower $L_A$ in LL results in reduced transpiration, and avoidance of excessive desiccation. De Lucia et al. (2000) found that for *P. ponderosa*, higher HV was associated with adaptation to dry conditions.

Although it was not measured in this study, it is possible that species differences in root distribution could be an important hydraulic architecture trait contributing to differential drought tolerance. Gholz et al. (1986) reported that in 27-year-old SL, about 80% of total root biomass was found in the top 0.1 m, and only 10% was present below 0.5 m soil depth. On the other hand, Addington et al. (2006) reported that for 44-year-old LL, ~32% of the total roots accumulated in the top 0.2 m soil depth and about 44% below 0.6 m soil depth. This more even root distribution of LL with depth could be an adaptation to more xeric habitats, allowing LL to reach deeper zones in the soil profile. More research is needed to test this hypothesis by measuring root length distribution of both species cohabiting the same site.

In conclusion, this analysis of hydraulic architecture and tracheid allometry revealed several similarities between ma-

ture LL and SL trees. Tracheid allometry markedly changed between roots, trunk and branch sapwood, and tracheid lumen diameter was highly correlated with sapwood hydraulic conductivity. Vulnerability to cavitation was not different between species for sapwood of roots, branches or trunk. Higher sapwood to leaf area ratio and higher maximum sapwood-specific hydraulic conductivity in roots of LL were functional traits that may allow LL to dominate in drier soil microsites of the flatwoods of the southeast US coastal plain. SL, on the other hand, may be better equipped to dominate at the fringe of ponds and wetter zones due to its ability to produce aerenchyma under low oxygen condition when the water table rises (Fisher and Stone 1990).

**Acknowledgments**

The authors greatly acknowledge Dr J.C. Domec for his help with the vacuum soaking method and Mr Dan Schultz and Mr Lamar Courtney for their support of the field work. Special thanks go to Mr Fabian Hergenreder, Mr Cristóbal González and Mr Andres Susaeta for their help in field sampling and lab work, Mr Kenneth Carabantes for his help with tracheid measurements and Mr Alejandro Riveros for his help with SG measurements. Funding was provided by National Science Foundation award #0344029 and the Forest Biology Research Cooperative at the University of Florida.

**References**

Addington, R.N., L.A. Donovan, R.J. Mitchell, J.M. Vose, S.D. Pecot, S.B. Jack, U.G. Hacke, J.S. Sperry and R. Oren. 2006. Adjustments in hydraulic architecture of *Pinus palustris* maintain similar stomatal conductance in xeric and mesic habitats. Plant Cell Environ. 29:535–545.

Aumann, C.A. and E.D. Ford. 2002. Modeling tree water flow as an unsaturated flow through a porous medium. J. Theor. Biol. 219:415–429.

Barnett, J.P. and R.M. Sheffield. 2005. Slash pine: characteristics, history, status and trends. *In* Slash Pine: Still Growing and Growing! Eds. E.D. Dickens, J.P. Barnett, W.G. Hubbard and E.L. Jokela. Proceedings of the Slash Pine Symposium, pp 1–6.

Burgess, S.S.O., J. Pittermann and T.E. Dawson. 2006. Hydraulic efficiency and safety of branch xylem increases with height in *Sequoia sempervirens* (D. Don) crowns. Plant Cell Environ. 29:229–239.

Čermák, J., J. Kučera and N. Nadezhdina. 2004. Sap flow measurements with two thermodynamic methods, flow integration within trees and scaling up from sample trees to entire forest stands. Trees Struct. Funct. 18:529–546.

Christensen-Dalsgaard, K.K., A.R. Ennos and M. Fournier. 2007. Changes in hydraulic conductivity, mechanical properties, and density reflecting the fall in strain along the lateral roots of two species of tropical trees. J. Exp. Bot. 58:4095–4105.

Comstock, G.L. 1970. Directional permeability of softwood. Wood Fiber 1:283–289.

Davis, S.D., J.S. Sperry and U.G. Hacke. 1999. The relationship between xylem conduit diameter and cavitation caused by freezing. Am. J. Bot. 86:1367–1372.

De Lucia, E.H., H. Maherali and E.V. Carey. 2000. Climate-driven changes in biomass allocation in pines. Global Change Biol. 6:587–593.

Domec, J.C. and B.L. Gartner. 2001. Cavitation and water storage capacity in bole xylem segments of mature and young Douglas-fir trees. Trees 15:204–214.

Domec, J.C., F.C. Meinzer, B.L. Gartner and D. Woodruff. 2005. Transpiration-induced axial and radial tension gradients in trunks of Douglas-fir trees. Tree Physiol. 26:275–284.

Domec, J.C., B. Lachenbruch and F.C. Meinzer. 2006*a*. Bordered pit structure and function determine spatial patterns of air-seeding thresholds in xylem of Douglas-fir (*Pseudotsuga menziesii*, Pinaceae) trees. Am. J. Bot. 93:1588–1600.

Domec, J.C., F.G. Scholz, S.J. Bucci, F.C. Meinzer, G. Goldstein and R. Villalobos-Vega. 2006*b*. Diurnal and seasonal variation in root xylem embolism in tropical savanna woody species: impact on stomatal control of plant water status. Plant Cell Environ. 29:26–35.

Duncan, P.D., T.L. White and G.R. Hodge. 1996. First-year freeze hardiness of pure species and hybrid taxa of *Pinus elliottii* (Engelman) and *Pinus caribaea* (Morelet). New Forest 12:223–241.

Ewel, J.J. 1990. Introduction. *In* Ecosystems of Florida. Eds. R.L. Myers and J.J. Ewel. University of Central Florida Press, Orlando, FL, p 3–10.

Fisher, H.M. and E.L. Stone. 1990. Air-conducting porosity in slash pine roots from saturated soils. For. Sci. 36:18–33.

Gaston, L., P. Nkedi-Kizza, G. Sawka and P.S.C. Rao. 1990. Spatial variability of morphological properties at a Florida flatwoods site. Soil Sci. Soc. Am. J. 54:527–533.

Gee, G.W. and J.W. Bauder. 1986. Particle-size analysis. *In* Methods of soil analysis. Part 1. Ed. A. Klute, 2nd ed. Agron. Monogr. 9. ASA and SSSA, Madison, WI, p 383–411.

Gholz, H.L., L.C. Hendry and W.P. Cropper. 1986. Organic-matter dynamics of fine roots in plantations of slash pine (*Pinus elliottii*) in north Florida. Can. J. For. Res. 16:529–538.

Gonzalez-Benecke, C.A. 2009. Interactions between xylem structure and water relations of southern pines. Gainesville, FL, USA, University of Florida, PhD dissertation.

Hacke, U.G., J.S. Sperry, B.E. Ewers, D.S. Ellsworth, K.V.R. Schäfer and R. Oren. 2000*a*. Influence of soil porosity on water use in *Pinus taeda*. Oecologia 124:495–505.

Hacke, U.G., J.S. Sperry and J. Pittermann. 2000*b*. Drought experience and cavitation resistance in six desert shrubs of the Great Basin, Utah. Basic Appl. Ecol. 1:31–41.

Hacke, U.G., J.S. Sperry, W.T. Pockman, S.D. Davis and K.A. McCulloh. 2001. Trends in wood density and structure are linked to prevention of xylem implosion by negative pressure. Oecologia 126:457–461.

Hacke, U.G., J.S. Sperry and J. Pittermann. 2004. Analysis of circular bordered pit function. II. Gymnosperm tracheids with torus-margo pit membranes. Am. J. Bot. 91:386–400.

Hatton, T.J., S.J. Moore and P.H. Reece. 1995. Estimating stand transpiration in a *Eucalyptus populnea* woodland with the heat pulse method: measurement errors and sampling strategies. Tree Physiol. 15:219–227.

Johnson, K., C. Maier and L. Kress. 2005. Quantifying root lateral distribution and turnover using pine trees with a distinct stable carbon isotope signature. Funct. Ecol. 19:81–87.

Kavanagh, K.L., B.J Bond, S.N. Aitken, B.L. Gartner and S. Knowe. 1999. Shoot and root vulnerability to xylem cavitation in four populations of Douglas-fir seedlings. Tree Physiol. 19:31–38.

Littell, R., G. Milliken, W. Stroup, R. Wolfinger and O Schabenberger. 2006. SAS system for mixed models. SAS Institute, Cary, NC, 814 pp.

Maherali, H. and E. De Lucia. 2000. Xylem conductivity and vulnerability to cavitation of ponderosa pine growing in contrasting climates. Tree Physiol. 20:859–867.

Maherali, H., C.F Moura, M.C. Caldeira, C.J. Willson and R.B. Jackson. 2006. Functional coordination between leaf gas exchange and vulnerability to xylem cavitation in temperate forest trees. Plant Cell Environ. 29:571–583.

Martin, T.A., K.J. Brown, J. Cermak, R. Ceulemans, J. Kucera, F.C. Meinzer, J.S. Rombold, D.G. Sprugel and T.M. Hinckley. 1997. Crown conductance and tree and stand transpiration in a second-growth *Abies amabilis* forest. Can. J. For. Res. 27:797–808.

Martinez-Vilalta, J., E. Prat, I. Oliveras and J. Pinol. 2002. Xylem hydraulic properties of roots and stems of nine Mediterranean woody species. Oecologia 133:19–29.

Matamala, R., M.A. Gonzalez-Meler, J.D. Jastrow, R. Norby and W.H. Schlesinger. 2003. Impacts of fine root turnover on forest NPP and soil C sequestration potential. Science 302:1385–1387.

Murthy, R. and P.M. Dougherty. 1997. Estimating foliage area of loblolly pine shoots. For. Sci. 43:299–303.

Niinemets, U., D.S. Ellsworth, A. Lukjanova and M. Tobias. 2001. Site fertility and the morphological and photosynthetic acclimation of *Pinus sylvestris* needles to light. Tree Physiol. 21:1231–1244.

Pammenter, N.W. and C. Vander Willigen. 1998. A mathematical and statistical analysis of the curves illustrating vulnerability of xylem to cavitation. Tree Physiol. 18:589–593.

Peet, R.K. 2006. Longleaf pine ecosystems: ecology, management, and restoration. Eds. S. Jose, E. Jokela and D. Miller. Springer, New York, p 51–94.

Pittermann, J. and J.S. Sperry. 2003. Tracheid diameter determines the extent of freeze–thaw induced cavitation in conifers. Tree Physiol. 23:907–914.

Pittermann, J., J.S. Sperry, U.G. Hacke, J.K. Wheeler and E. Sikkema. 2006*a*. Inter-tracheid pitting and the hydraulic efficiency of conifer wood: the role of tracheid allometry and cavitation protection. Am. J. Bot. 93:1105–1113.

Pittermann, J., J.S. Sperry, J.K. Wheeler, U.G. Hacke and E. Sikkema. 2006*b*. Mechanical reinforcement against tracheid implosion compromises the hydraulic efficiency of conifer xylem. Plant Cell Environ. 29:1618–1628.

Pockman, W.T. and J.S. Sperry. 2000. Vulnerability to cavitation and the distribution of Sonoran Desert vegetation. Am. J. Bot. 87:1287–1299.

Powell, T.L., G. Starr, K.L. Clark, T.A. Martin and H.L. Gholz. 2005. Ecosystem and understory water and energy exchange for a mature, naturally regenerated pine flatwoods forest in north Florida. Can. J. For. Res. 35:1568–1580.

Powell, T.L., H.L. Gholz, K.L. Clark, G. Starr, W.P. Cropper, Jr. and T.A. Martin. 2008. Carbon exchange of a mature naturally-regenerated pine forest in north Florida. Global Change Biol. 14:2523–2538.

Robertson, G., J. Olson, P. Allen, B. Chan and R. Seth. 1999. Measurement of fiber length, coarseness, and shape with the fiber quality analyzer. TAPPI J. 82:93–98.

Ruzin, S.E. 1999. Plant microtechnique and microscopy. Oxford University Press, New York, 336 pp.

Santiago, L.S., G. Goldstein, F.C. Meinzer, J. Fisher, K. Machado, D. Woodrduf and T. Jones. 2004. Leaf photosynthetic traits scale with hydraulic conductivity and wood density in Panamanian forest canopy trees. Oecologia 140:543–550.

Schaap, M.G., F.J. Leij and M. Th. Van Genuchten. 2001. Rosetta: a computer program for estimating soil hydraulic parameters with hierarchical pedotransfer functions. J. Hydrol. 251:163–176.

Schimleck, L.R., R.D. Jones, G.F. Peter, R.F. Daniels and A. Clark. 2004. Nondestructive estimation of tracheid length from sections of radial wood strips by near infrared spectroscopy. Holzforschung 58:375–381.

Simpson, W.T. 1993. Specific gravity, moisture content, and density relationship for wood. Gen. Tech. Rep. FPL-GTR-76. USDA Forest Service Forest Prod. Lab., Madison, WI, 13 pp.

Sperry, J.S. and N.Z. Saliendra. 1994. Intra- and inter-plant variation in xylem cavitation in *Betula occidentalis*. Plant Cell Environ. 17:1233–1241.

Sperry, J.S. and M.T. Tyree. 1988. Mechanism of water-stress induced xylem embolism. Plant Physiol. 88:581–587.

Sperry, J.S. and M.T. Tyree. 1990. Water-stress-induced xylem embolism in three species of conifers. Plant Cell Environ. 13:427–436.

Sperry, J.S., M.T. Tyree and J.R. Donnelly. 1988. Vulnerability of xylem to embolism in a mangrove vs. an inland species of Rhizophoraceae. Physiol. Plantarum 74:276–283.

Sperry, J.S., F.R. Adler, G.S. Campbell and J.P. Comstock. 1998. Limitation of plant water use by rhizosphere and xylem conductance: results from a model. Plant Cell Environ. 21:347–359.

Sperry, J.S., U.G. Hacke, R. Oren and J.P. Comstock. 2002. Water deficits and hydraulic limits to leaf water supply. Plant Cell Environ. 25:251–263.

Sperry, J.S., U.G. Hacke and J. Pittermann. 2006. Size and function in conifer tracheids and angiosperm vessels. Am. J. Bot. 93:1490–1500.

Spicer, R. and B.L. Gartner. 1998*a*. How does a gymnosperm branch assume the hydraulic status of a main stem when it takes over as leader? Plant Cell Environ. 21:1063–1070.

Spicer, R. and B.L. Gartner. 1998*b*. Hydraulic properties of Douglas-fir (*Pseudotsuga menziesii*) branches and branch halves with reference to compression wood. Tree Physiol. 18:777–784.

Spicer, R. and B.L. Gartner. 2001. The effects of cambial age and position within the stem on specific conductivity in Douglas-fir sapwood. Trees 15:222–229.

Tyree, M.T. and F.W. Ewers. 1991. The hydraulic architecture of trees and other woody plants. New Phytol. 119:345–360.

Tyree, M.T. and M.H. Zimmermann. 2002. Xylem structure and the ascent of sap. Second Edition. Springer, Berlin, 283 pp.

White, F.M. 1991. Viscous fluid flow. McGraw-Hill, New York, 736 pp.

Whitehead, D., W.R.N. Edwards and P.G. Jarvis. 1984. Conducting sapwood area, foliage area, and permeability in mature trees of *Picea sitchensis* and *Pinus contorta*. Can. J. For. Res. 14:940–947.

Zwieniecki, M.A. and N.M. Holbrook. 2000. Bordered pit structure and vessel wall surface properties—implications for embolism repair. Plant Physiol. 123:1015–1020.